A novel technique for measuring the reflection coefficient of sound absorbing materials

H-E. de Bree[1], F.J.M. van der Eerden[2], J.W. van Honschoten[1]
[1] Dep. of Electrical Eng. (TT), [2] Dep. of Mechanical Eng. (TMK), University of Twente, The Netherlands
E-mail: f.j.m.vandereerden@wb.utwente.nl

Abstract

A new method to measure the acoustic behaviour of sound absorbing material in an impedance tube is presented. The method makes use of a novel particle velocity sensor, the microflown, and a microphone. The so-called p·u method is compared to three other methods of which the two microphone technique is well known. It is shown that the combination of a microphone and a microflown provides direct information on the acoustic impedance, the sound intensity and the sound energy density. The experimental results are compared to the results obtained with the conventional impedance tube measurements. To be able to repeat the measurements in a reliable way a well described test sample with a quarter-wave resonator is used. Furthermore it is shown that the viscothermal effects on the wave propagation are important, i.e. for the quarter-wave resonator and to a lesser extent for the impedance tube itself.

1. Introduction

A number of measurement techniques can be used to quantify the sound absorbing behaviour of porous materials. In general one is interested in one of the following properties: the sound absorption coefficient α, the reflection coefficient *R*, or the surface impedance *Z*. The techniques can be divided into three categories:

- Reverberant field methods
- Free field methods
- Impedance tube methods (Kundt's tube)

The impedance tube technique is the topic of the present investigation (see Figure 1).

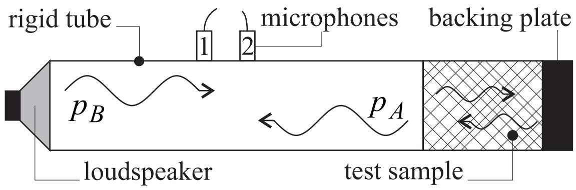

Figure 1 Outline of an impedance tube.

At one end of the impedance tube a loudspeaker is placed and at the other end a sample of the test material is placed. In the tube a standing wave pattern is established as a result of the forward, p_B, and backward, p_A, travelling waves. The frequency of the sound waves is kept low enough to assure plane propagating waves in the tube.

The first technique made use of the measured standing wave ratio (SWR) in the tube for a specific frequency. Next, in 1980 Chung and Blazer [1] presented a technique which is based on the transfer function of two fixed microphones (see Figure 1). The standing wave pattern in their case is built up from a broadband stationary noise signal. With the measured transfer function the incident and reflected waves are separated mathematically. This leads to the reflection coefficient *R* of the sample for the complete frequency band. The normal impedance Z_n and the sound absorption coefficient α can be derived as well. The transfer function technique, here called the **2p method**, has proven to be efficient and reliable (see ISO 10534-2 1998).

With the development of the first acoustic particle velocity sensor, the microflown, alternative measurement techniques become possible in the impedance tube. These techniques are presented in section 4:

- The **2u method**
- The **u/p method**
- The **p·u method**

The two latter methods make use of the combination of a microphone and a microflown to determine the acoustic behaviour of a sound absorbing sample. The p·u method is a new technique and makes use of the measured sound intensity and sound energy density. By using the p·u method a good indication of the quality of the measured sound intensity and energy density is obtained. The first results of the p·u method are presented and compared to the three other methods.

Furthermore it will be shown that the combination of a microflown and a microphone, in a slightly different set-up, is useful to calibrate the microflown with respect to a calibrated microphone (see section 5.1). In section 5.2 the experimental results of the different methods are mutually compared. Furthermore they are compared to the theoretical sound absorption coefficient of a well described sample with a quarter-wave resonator. In this way the measurements can be repeated in a reliable way.

First the microflown is described in section 2. The theory for the viscothermal wave propagation in the impedance tube and the resonator is given in section 3.

2. The microflown

The microflown (or µ-flown) was developed by De Bree et al. [2]. Instead of pressure the microflown measures the average acoustic particle velocity of a small finite volume of air. The measurement principle of the microflown is based on the temperature difference between two resistive sensors which are 40 µm apart as shown in Figure 2 and Figure 3. The microflown consists of two cantilevers of silicon nitride with a platinum pattern on top. The size of the cantilevers is 800×40×1 µm (l×w×h).

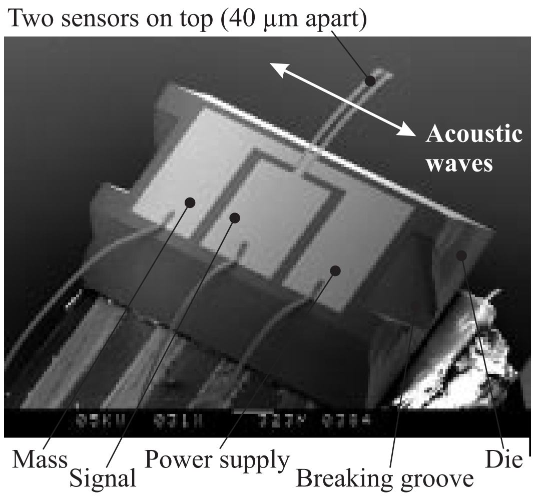

Figure 2 Photograph of the microflown.

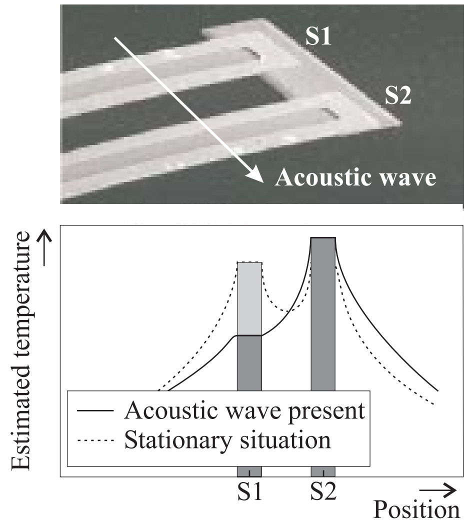

Figure 3 Photograph of the sensors on top and estimated temperature profile.

It follows from Figure 3 that a travelling acoustic wave causes movements of the air and as a result heat is transferred from one sensor to the other (harmonically for a single frequency). This causes a difference in temperature of the two sensors. The temperature difference between both sensors causes a differential electrical resistance variation which is measured. To realise a temperature difference that is high enough to be able to measure the resistance variation the sensors are heated by a DC current up to about 400-600 degrees Kelvin.

The sensitivity of the microflowns shows approximately a first order low pass behaviour. The corner frequency, above which the sensitivity drops 6 dB per octave, is between 300 Hz and 1kHz. More practical characteristics of the microflown are:

- The directional sensitivity varies cosine-like (as in a figure of eight). Therefore the sensors can be aligned accurately by hand.
- The absence of a resonance mechanism.
- The low costs due to simplicity and batch size.
- The ability to measure the particle velocity in the near field where the sound intensity technique with two closely spaced microphones breaks down.
- The vulnerability of the two sensors. A protective package may be used (see also section 4).
- The microflown has to be positioned outside a boundary layer whereas a microphone is usually flush-mounted in the impedance tube wall.

A new design of the microflowns is shown in Figure 4. The cantilevers of the two sensors are supported at both sides for extra stability. Furthermore, the sensors are smaller to gain extra sensitivity. For the sake of completeness also a microflown with three pairs of sensors is depicted in Figure 5 which measures the three orthogonal velocity components. In this way the measurement of the sound intensity vector becomes relatively easy.

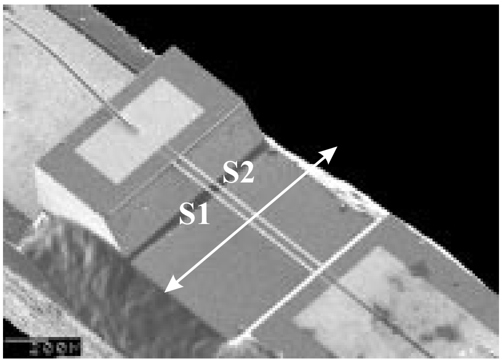

Figure 4 A bridge-type microflown.

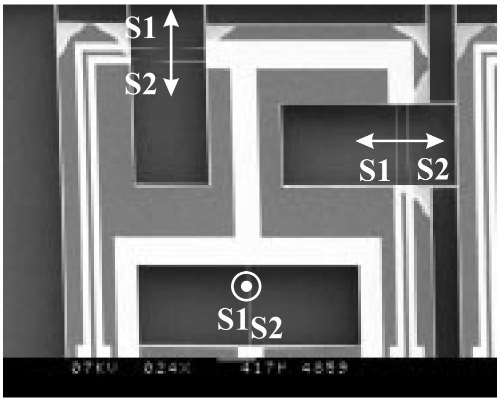

Figure 5 A microflown for three dimensions.

3. Viscothermal wave propagation

3.1 The wave propagation coefficient

In small tubes the wave propagation is affected by the viscosity and the thermal conductivity of the fluid. There is a variety of literature on the viscothermal wave propagation. Tijdeman [3] and Beltman [4] give a complete overview of the different analytical solutions. It is shown there that the approach of Zwikker and Kosten leads to an efficient and accurate solution. They assumed a constant pressure across the tube cross-section and included the effects of inertia, compressibility, viscosity and thermal conductivity of the fluid. For a prismatic tube as shown in Figure 6 the harmonic pressure perturbation $p(x)$ and the harmonic velocity perturbation $u(x)$ are given by (1) and (2).

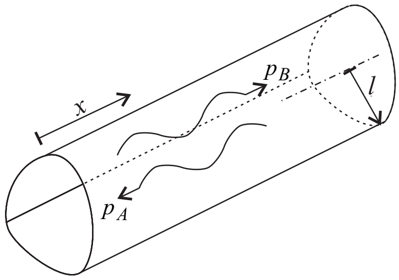

Figure 6 A prismatic tube.

$$p(x) = p_A\, e^{\Gamma k x} + p_B\, e^{-\Gamma k x} \tag{1}$$

$$u(x) = \frac{G}{\rho_0 c_0}\left(p_A\, e^{\Gamma k x} - p_B\, e^{-\Gamma k x}\right) \tag{2}$$

where $u(x)$ is the averaged velocity over the cross-section so that a one-dimensional model arises. The viscothermal effects are present in the wave propagation coefficient Γ.

The solution of Zwikker and Kosten was rewritten in a dimensionless form by Tijdeman. In the so-called 'low reduced frequency model' four dimensionless parameters, s , k_r, σ and γ characterise the wave propagation (see Appendix: List of Symbols). The shear wave number s is a measure for the ratio between the inertial and viscous forces and can be seen as an unsteady Reynolds number.

$$s = l\sqrt{\frac{\rho_0 \omega}{\mu}} \tag{3}$$

For small values of s the viscous effects are dominant. In that case a tube is called 'narrow'. For s » 1 the tube is called 'wide'. Beltman has demonstrated that for most acoustic problems the low reduced frequency model is sufficient. Compared to other models, like the simplified Navier Stokes model, the low reduced frequency model is a relatively simple one.

The wave propagation coefficient Γ is a complex number, i.e. $\Gamma = \mathrm{Re}(\Gamma) + i\,\mathrm{Im}(\Gamma)$, where $c_0 / \mathrm{Im}(\Gamma)$ represents the effective phase velocity and $\mathrm{Re}(\Gamma)$ represents the attenuation of a propagating wave. It is noticed that Γ is a function of the shear wave number s and therefore a function of the frequency.

In the present investigation s » 1 applies for the tubes. As a result a first order approximation of the low reduced frequency solution can be used. For large values of the shear wave number s, i.e. for 'wide' tubes, the propagation coefficient Γ can be estimated according to Kirchhoff:

$$\Gamma = i + \frac{i+1}{\sqrt{2}}\left(\frac{\gamma - 1 + \sigma}{s\sigma}\right) \tag{4}$$

The accompanying velocity coefficient G is:

$$G = -\frac{i}{\Gamma} \tag{5}$$

From (4) it can be seen that both viscous and thermal effects are included. These effects are taken into account for the impedance tube and the quarter-wave resonator.

3.2 The reflection coefficient

The amplitudes p_B and p_A of the forward and backward travelling waves in the tube are governed by the boundary conditions at both ends of the tube. In Figure 7 the possible boundary conditions are shown.

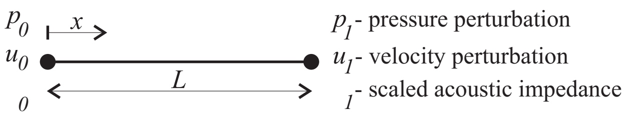

Figure 7 One-dimensional tube and possible boundary conditions.

For a tube terminated with a sound absorbing material an impedance condition can be used. The specific acoustic impedance is denoted by Z_a and relates the pressure, at a specific position or at a surface, to the normal velocity. In the present investigation the impedance is scaled to the characteristic impedance of a travelling plane wave. The characteristic impedance of a *freely* plane propagating wave is $\rho_0 c_0$. However, in a duct where the viscothermal wave propagation is included the characteristic impedance is $-\rho_0 c_0/G$. Therefore the scaled (dimensionless) impedance ζ becomes:

$$\zeta(x) = \frac{-G}{\rho_0 c_0} Z_a(x) = \frac{-G}{\rho_0 c_0} \frac{p(x)}{u(x)} \tag{6}$$

More convenient quantities for sound absorbing materials are the reflection R and the sound absorption coefficient α. The reflection coefficient is the ratio between the reflected and the incident wave and by using equation (1) gives:

$$R(x) = \frac{p_A e^{\Gamma k x}}{p_B e^{-\Gamma k x}} \tag{7}$$

The acoustic energy in a plane wave is proportional to the squared amplitude of the pressure. Therefore $|R|^2$ is the ratio of the reflected energy to the incident energy.

The sound absorption coefficient α is defined as

$$\alpha = 1 - |R|^2 \tag{8}$$

where α is the fraction of the incident energy which is dissipated.

With known amplitudes p_A and p_B the impedance $\zeta(x)$ can be determined and with the use of the definition of the reflection coefficient $R(x)$ one can derive:

$$R(x) = \frac{\zeta(x) - 1}{\zeta(x) + 1} \tag{9}$$

3.3 A quarter-wave resonator

A sample with a single tube, a quarter-wave resonator, is placed at the end of an impedance tube with a square cross-section. The sample is depicted in Figure 8.

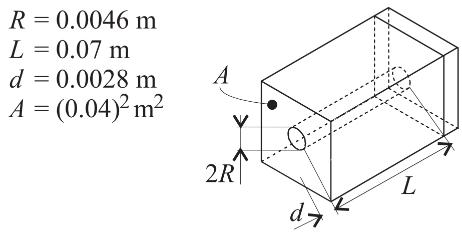

Figure 8 Sample with a quarter-wave resonator.

Due to inlet effects the effective length L_{eff} of the resonator is longer than the actual length L. The end correction d for a tube centrally located in another tube with radius R_2 is [5]:

$$d = \frac{8R}{3\pi}\left(1 - 1.25 \, {}^{R}\!/_{R_2}\right); \qquad \text{with } {}^{R}\!/_{R_2} < 0.6 \tag{10}$$

For the square cross-section the radius R_2 is estimated by $R_2 = 0.04$m.

With the use of (1), (2) and (6) the impedance at the entrance of the resonator is deduced:

$$\zeta(x{=}0) = \frac{\cosh(\Gamma k L_{eff})}{\sinh(\Gamma k L_{eff})} \tag{11}$$

The impedance of the sample *itself* is calculated by using a reference frame across the surface of the sample. The pressure and the mass flow on the left- and right-hand side of the reference frame are equal, so one has:

$$\zeta_{sample} = \left(\frac{\pi R^2}{A}\right)^{-1} \cdot \zeta(x{=}0) \tag{12}$$

4. The impedance tube

4.1 Experimental set-up

The impedance tube is sketched in Figure 9. The four methods are shortly discussed in the next sections: the 2p, 2u, p/u and the p·u method.

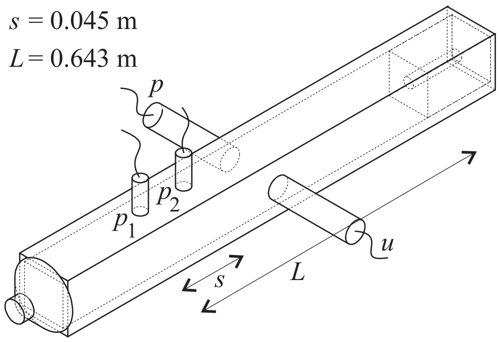

Figure 9 Impedance tube and sensor positions.

The microphone positions for the 2p method are indicated by p_1 and p_2. The same positions are used for the 2u method but then two microflowns are used. For the p/u and the p·u method the positions of the microphone and the microflown are indicated by *p* and *u*, respectively. Notice that for the latter two methods there is no separation distance *s* and that the distance to the sample *L* is different (L = 0.407 m). The microphones for the 2p method are ¼ inch Kulites. For the p/u and p·u method a ½ inch B&K microphone and a ½ inch ICP μ-flown Technologies is used.

4.2 The 2p method

The measured transfer function is:

$$H_{2p} = \frac{p_2}{p_1} = \frac{S_{p_2 p_1}}{S_{p_1 p_1}} \tag{13}$$

where p_2 and p_1 are the pressures in the frequency domain, S_{p2p1} is the cross-spectrum and S_{p1p1} is the auto-spectrum. The transfer function H_{2p} can be measured directly with a two channel FFT analyser. With the theory for the one dimensional wave propagation as presented in section 3 one can derive the reflection coefficient at the surface of the sample, i.e. at $x = L$:

$$R(x{=}L) = \frac{H_{2p} - e^{-\Gamma k s}}{-H_{2p} + e^{\Gamma k s}} \cdot \frac{e^{\Gamma k L}}{e^{-\Gamma k L}} \tag{14}$$

4.3 The 2u method

The measured transfer function is:

$$H_{2u} = \frac{u_2}{u_1} = \frac{S_{u_2 u_1}}{S_{u_1 u_1}} \tag{15}$$

With H_{2u} and the theory presented in section 3 the reflection coefficient *R* becomes:

$$R(x{=}L) = \frac{H_{2u} - e^{-\Gamma k s}}{H_{2u} - e^{\Gamma k s}} \cdot \frac{e^{\Gamma k L}}{e^{-\Gamma k L}} \tag{16}$$

4.4 The p/u method

The transfer function $H_{p/u}$ is measured in the frequency domain according to:

$$H_{p/u} = \frac{p}{u} = \frac{S_{pu}}{S_{uu}} \tag{17}$$

If the microphone and the microflown are located at $x = 0$ then the impedance at the sample at $x = L$, is:

$$\zeta(x{=}L) = \frac{H_{p/u}\cosh(\Gamma k L) - \rho_0 c_0 \sinh(\Gamma k L)}{\rho_0 c_0 \cosh(\Gamma k L) + H_{p/u}\sinh(\Gamma k L)} \tag{18}$$

Equation (18) is obtained by using the theory for the one dimensional wave propagation.

Acoustic impedance measurements with the p/u method were first performed by Schurer in 1996 directly in the throat of a horn [6].

4.5 The p·u method

By measuring the sound intensity and the sound energy density (at $x = 0$) it is possible as well to derive the amplitude reflection coefficient $|R|$. Fahy [7] shows that in a tube the mean speed of the energy transport $\bar{c}_e$ is the ratio between the mean intensity and the mean energy density:

$$\bar{c}_e = \frac{\bar{I}}{\bar{E}} = c_0 \frac{1 - |R|^2}{1 + |R|^2} \tag{19}$$

So the reflection coefficient $|R|$ at the surface of a sample (at $x = L$, see also equation (7)), and by taken into account the viscothermal losses in the impedance tube, is:

$$R^2 = \frac{\bar{E} c_0 - \bar{I}}{\bar{E} c_0 + \bar{I}} \cdot \left| \frac{e^{\Gamma k L}}{e^{-\Gamma k L}} \right|^2 \tag{20}$$

The time averaged energy density is defined as:

$$\overline{E} = \frac{1}{4}\rho_0\, u\, u^* + \frac{p\, p^*}{4\rho_0\, c_0{}^2} \tag{21}$$

and the active intensity (also time averaged) is:

$$\bar{I} = \frac{1}{2}\mathrm{Re}\{pu^*\} \tag{22}$$

where p and u are complex amplitudes in the frequency domain.

Using a two channel FFT analyser one has:

$$\overline{E} = \frac{1}{2}\rho_0\, S_{uu} + \frac{1}{2\rho_0 c_0{}^2} S_{p\,p} \tag{23}$$

$$\bar{I}_{active} = \mathrm{Re}\{S_{pu}\} \tag{24}$$

With (23), (24) and (20) the value of $|R|$ can be determined.

The results of the new p·u method are compared to the results of the other methods in section 5.2.

5. Experimental results

Before the reflection coefficient R (or the sound absorption coefficient α) of a sample with a quarter-wave resonator is measured the sensors are calibrated. The procedure and the calibration results for the combination of a microphone and a microflown are described in the following section.

5.1 Calibration results

For the calibration of the *combination* of the microphone and the microflown the position of both sensors is indicated in Figure 10.

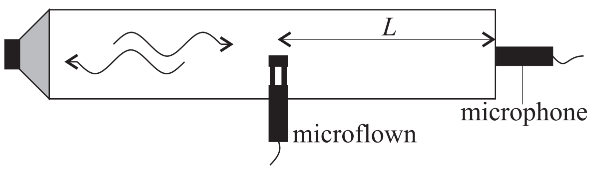

Figure 10 Set-up for the calibration measurements.

The measured and theoretical transfer function $H_{u/p}$ are given in Figure 11. A minimum occurs when the velocity has a minimum value at the location of the microflown. The right-hand side of the impedance tube is approximately acoustically hard (ζ(L) = 1000) so that there is always a pressure maximum.

$$H_{u/p} = \frac{-G}{\rho_0 c_0}\left(\sinh(\Gamma kL) + \frac{\cosh(\Gamma kL)}{\zeta(x{=}L)}\right) \tag{25}$$

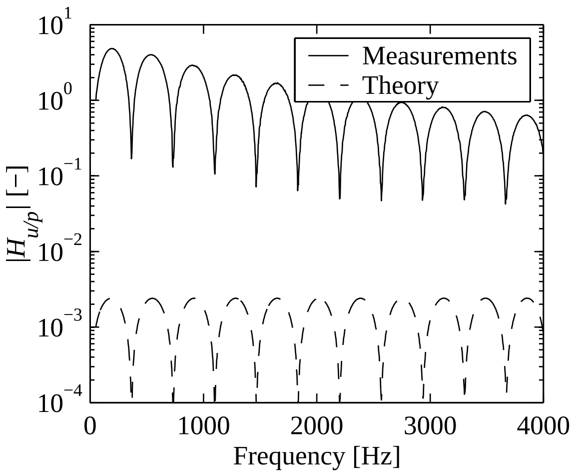

Figure 11 Transfer function $H_{u/p}$ (magnitude).

From the measured and theoretical values (theory: without gain) a correction function is obtained as a function of the frequency. The difference for the amplitude and the phase is given in the Figure 12 and 13. As a first approach a third order polynomial is used for the final interpolated correction.

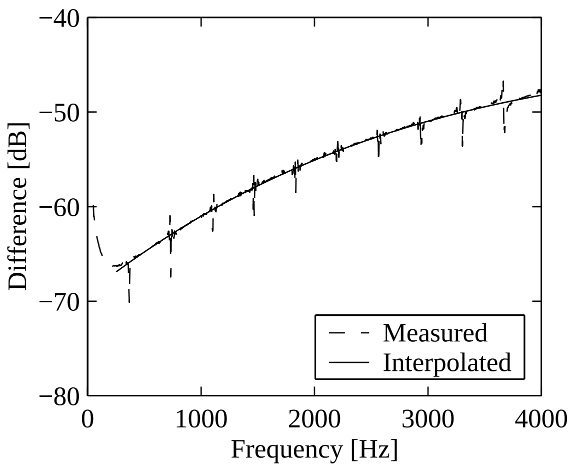

Figure 12 Amplitude difference in dB.

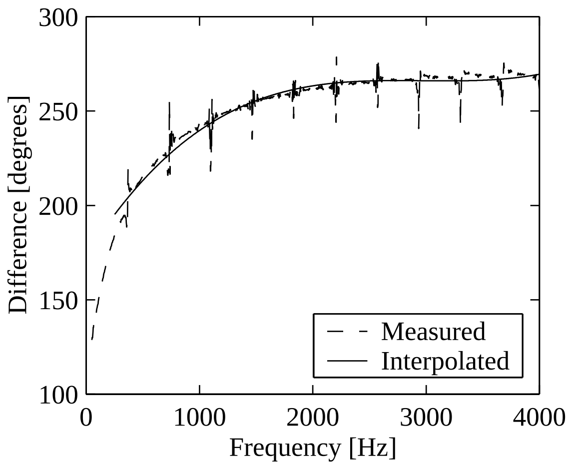

Figure 13 Phase difference in degrees.

For the present tests the measured transfer function $H_{u/p}$ is corrected in the following way:

$$20\log\left|\tilde{H}_{u/p}\right| \rightarrow 20\log\left|H_{u/p}\right| + \text{Correction} \quad [\text{dB}] \quad (26)$$

$$\arg(\tilde{H}_{u/p}) \rightarrow \arg(H_{u/p}) + \text{Correction} \quad [\text{deg}] \quad (27)$$

5.2 A sample with a quarter-wave resonator

The measurement set-up is in Figure 9 and the results are presented in the Figures 14, 15 and 16. For the results with the 2u method reference is made to [8] where it is shown that the 2u method provides the same results as the 2p method.

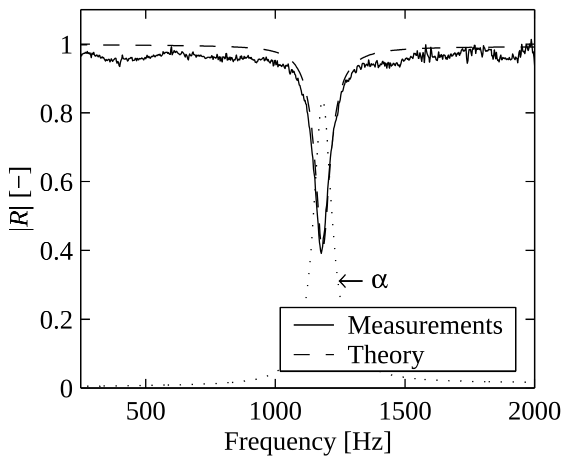

Figure 14 Reflection coefficient (magnitude) using the 2p method.

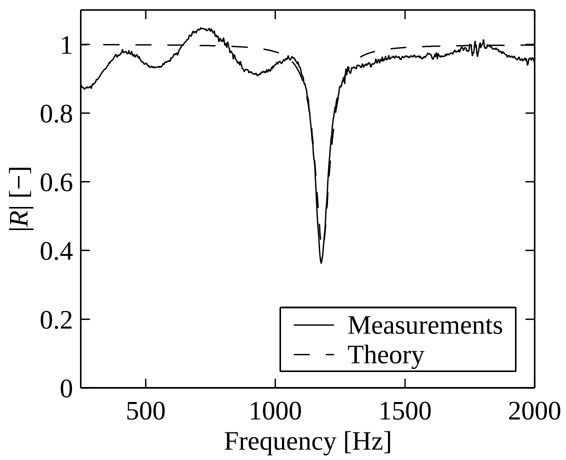

Figure 15 Reflection coefficient (magnitude) using the p/u method.

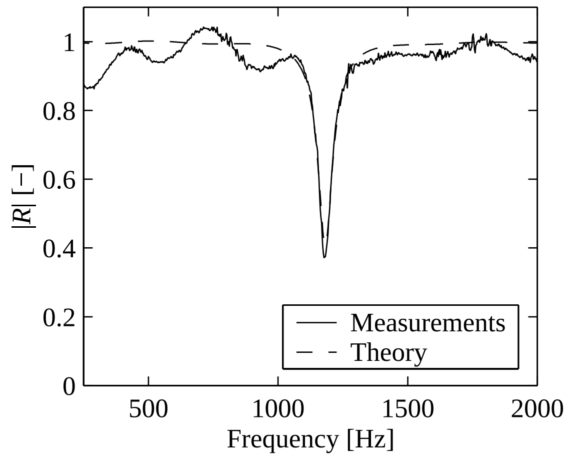

Figure 16 Reflection coefficient (magnitude) using the p·u method.

The figures show that the three methods provide identical results for the frequency range where the quarter-wave resonator is effective, i.e. from 1000 to 1400 Hz. For the lower frequency range the u/p and the p·u method are less accurate. This may be improved with a more accurate calibration of the transfer function $H_{u/p}$. It is noted that the phase-calibration can be performed with the microphone flush mounted. In this way the microphone shows the same phase-response behaviour because the incident sound field is the same as for the experiments with a sound absorbing sample. In this respect it has to be remarked that the calculation of R for an acoustic hard wall is very sensitive to measurement inaccuracies.

The figures also reveal that the theoretical model of section 3 predicts the acoustic behaviour very accurately for the complete frequency range. This indicates that the viscothermal wave propagation is correctly modelled.

It has been shown that the p·u method is a practical technique to measure the reflection coefficient, the sound intensity and the sound energy density. Next, the transmission loss in an impedance tube and the sound intensity vector and the energy density outside a pipe can be measured.

6. Conclusions

Four methods to measure the acoustic behaviour of sound absorbing material in an impedance tube have been presented: the 2p, 2u, p/u and the p·u method and the results have been mutually compared Three methods make use of a novel particle velocity sensor, the microflown. It has been shown that the microflown can be an attractive alternative to microphones. Furthermore, the combination of a microphone and a microflown provides direct information on the acoustic impedance, the sound intensity and the sound energy density. Besides it has been demonstrated that for narrow tubes the viscothermal effects on the wave propagation are important, i.e. for a quarter-wave resonator and to a lesser extent for the impedance tube itself.

Acknowledgements

The authors would like to thank W.F. Druyvesteyn and G.J.M. Krijnen for their fruitful discussions. The comments of H. Tijdeman, R.M.E.J. Spiering, P.J.M. van der Hoogt and T.G.H. Basten are gratefully acknowledged. This research is supported by the Dutch Technology Foundation (STW).

References

1. Chung, J.Y., Blaser, D.A. Transfer function method of measuring in-duct acoustic properties. I. Theory, *J. of the Acoust. Society of America*, **68**(3), 907-913 (1980)
2. Bree, H-E. de, Leussink, P.J., Korthorst, M.T., Jansen, H.V., Lammerink, T., Elwenspoek, M. The Microflown: a novel device measuring acoustical flows, *Sensors and Actuators A*, **54**, 552-557 (1996)
3. Tijdeman, H. On the propagation of sound waves in cylindrical tubes, *J. of Sound and Vibration*, **39**(1), 1-33 (1975)
4. Beltman, W.M. Viscothermal wave propagation including acousto-elastic interaction, part I: theory, *J. of Sound and Vibration* **227**(3), 555-586 (1999)
5. Bies, D.A., Hansen, C.H. *Engineering Noise Control, theory and practice*, E&FN SPON, London (1996)
6. Schurer, H., Annema, P., de Bree, H-E., Slump, C.H., Herman, O. Comparison of two methods for measurements of horn input impedance, *J. Audio Eng. Society*, **44**, 649 (1996)
7. Fahy, F.J. *Sound intensity*, E&FN SPON, London (1995)
8. Eerden, F.J.M., de Bree, H-E., Tijdeman, H. Experiments with a new acoustic particle velocity sensor in an impedance tube, *Sensors and Actuators A*, **69**, 126-133 (1998)

Appendix: List of Symbols

A	Surface	[m^2]
c_0	Undisturbed speed of sound	[m/s]
$\bar{c}_e$	Mean speed of energy transport	[m/s]
C_p	Specific heat at constant pressure	[J/kgK]
C_V	Specific heat at constant volume	[J/kgK]
d	Length increment due to inlet effects	[m]
$\overline{E}$	Time averaged sound energy density per unit volume	
G	Parameter for the velocity $u(x)$	
H_{2p}	Transfer function of two microphones	
$i=\sqrt{-1}$	Imaginary number	
$\bar{I}$	Time averaged or mean sound intensity	[J/(m^{2}s)]
$k=\omega/c_0$	Wave number	[m^{-1}]
$k_r=l\,\omega/c_0$	Reduced frequency	
$l=R$	Half the characteristic length of the cross-section	[m]
L	Length of a tube	[m]
p	Pressure perturbation	[Pa]
R	Reflection coefficient	
R	Radius	[m]
$s=l\sqrt{\omega\rho_0/\mu}$	Shear wave number	
s	Distance between two microphones	[m]
S_{pu}	Cross-spectrum	
S_{pp}	Auto-spectrum	
t	Time	[s]
T	Kinetic energy per unit volume	[J/m^3]
u	Particle velocity perturbation	[m/s]
U	Potential energy per unit volume	[J/m^3]
x	Cartesian co-ordinate	[m]
Z_a	Acoustic impedance	[kg/(m^{2}s)]
α	Sound absorption coefficient	
$\gamma=C_p/C_V$	Ratio of specific heats	
Γ	Viscothermal wave propagation coefficient	
λ	Thermal conductivity	[J/msK]
μ	Dynamic viscosity	[Pa s]
ρ_0	Mean density	[kg/m^3]
$\sigma=\sqrt{\mu C_p/\lambda}$	Square root of the Prandtl number	
ω	Angular frequency	[rad/s]
Ω	Porosity of a surface	
ζ	Acoustic dimensionless impedance	
Re{ }	Real part	
Im{ }	Imaginary part	
| |	Amplitude	
*	Complex conjugate	